Interplay between the orbital and magnetic order in monolayer $La_{1-x}Sr_{1+x}MnO_4$ manganites

2007 J. Phys.: Condens. Matter 19 186223

(http://iopscience.iop.org/0953-8984/19/18/186223)

IOP PUBLISHING JOURNAL OF PHYSICS: CONDENSED MATTER

J. Phys.: Condens. Matter **19** (2007) 186223 (17pp) doi:10.1088/0953-8984/19/18/186223

Interplay between the orbital and magnetic order in monolayer $La_{1-x}Sr_{1+x}MnO_4$ manganites

Krzysztof Rościszewski[1] **and Andrzej M Oleś**[1,2]

[1] Marian Smoluchowski Institute of Physics, Jagellonian University, Reymonta 4, PL-30059 Kraków, Poland
[2] Max-Planck-Institut für Festkörperforschung, Heisenbergstrasse 1, D-70569 Stuttgart, Germany

E-mail: roscis@if.uj.edu.pl and a.m.oles@fkf.mpg.de

Received 12 December 2006
Published 13 April 2007
Online at stacks.iop.org/JPhysCM/19/186223

Abstract

A two-dimensional model which describes e_g electrons in a monolayer of an undoped and half doped manganite $La_{1-x}Sr_{1+x}MnO_4$ is studied using correlated wavefunctions. The effective Hamiltonian takes into account the kinetic energy, the crystal field splitting between $x^2 - y^2$ and $3z^2 - r^2$ orbitals, and on-site Coulomb interactions for e_g electrons. They interact with $S = 3/2$ spins due to t_{2g} electrons, which are treated as frozen core spins. Furthermore, the model includes antiferromagnetic superexchange interaction between core spins, and the coupling between e_g electrons and Jahn–Teller modes. The model reproduces the antiferromagnetic order in the undoped $LaSrMnO_4$ compound, with occupied $3z^2 - r^2$ orbitals and elongated MnO_6 octahedra along the direction perpendicular to the Mn–O plane. In half doped $La_{0.5}Sr_{1.5}MnO_4$ manganite one finds robust chequerboard-like charge order using realistic parameters. However, the experimentally observed CE phase is more difficult to stabilize, and we discuss the necessary conditions to obtain it within the present model. Altogether, we conclude that the Jahn–Teller effect plays a crucial role in the entire regime of doping.

1. Introduction

Doped perovskite manganese oxides have attracted much attention not only because of colossal magnetoresistance (CMR), but also because of the rich variety of magnetic, orbital structural and charge order (CO) they display. The properties of doped manganites are still very puzzling and not completely understood, in spite of much effort both in theory and in experiment. Recently, their modelling became the focus in intense research activity in the theory of strongly correlated electron systems [1, 2].

The main difficulty in the theoretical description of this class of compounds is related to the simultaneous importance of numerous degrees of freedom, and early attempts to consider only some of them, such as for instance the Jahn–Teller (JT) effect supplemented by Hund's exchange but neglecting other on-site Coulomb interactions [1, 3], or considering only on-site Coulomb interaction U while neglecting Hund's exchange, or only the coupling to the lattice due to the JT effect [4], turned out to be insufficient to account for the experimental situation, in spite of their unquestionable successes in treating particular aspects [5, 6]. Only in the last decade it has been recognized that the JT interactions and the superexchange which occurs due to e_g electron excitations in the regime of large on-site Coulomb interactions support each other [7], and both are necessary to explain the magnetic and optical properties of undoped $LaMnO_3$ [8]. It is not surprising that the JT interactions play a role for the magnetism, as it is well known that in certain situations they modify the superexchange [9]. In addition, it has also been realized that the core t_{2g} electrons, even if localized (passive), play an essential role for the observed magnetic phases [10–12]. In short, one cannot argue that some of the above interactions are essential for the observed physical properties of manganites, while the others are only of secondary importance. The phase situation in this class of compounds is a result of a rather subtle balance between all these factors.

On the theoretical side, the multiband models and/or approaches based on the *ab initio* local density approximation (LDA) computations extended by either static corrections due to local Coulomb interaction U (LDA + U) [10, 13–15], or by dynamical mean field theory (LDA + DMFT method) [16], seem to provide the best available theoretical description of perovskite manganese oxides nowadays. The drawback of such approaches, however, is the multitude of unknown parameters which have to be independently estimated and/or the prohibitive cost of the computations. Under these circumstances it is far easier to identify the physical mechanisms responsible for particular types of order observed in doped manganites using well motivated and transparent microscopic models.

In the present paper we set up an effective model for itinerant e_g electrons which benefits from the above accumulated experience and includes all essential interactions present in monolayer manganites. In view of the large number of Hamiltonian parameters and the necessity to include numerous interactions (in a reasonably accurate manner), we adopt an effective model featuring only Mn sites (renormalized by the presence of surrounding oxygen ions). Thereby we do not aim to develop new concepts but rather to put together the elements tested in numerous earlier papers and to investigate which states result from a complete theoretical model when local electron correlations and the JT effect are both included. As the first step it is reasonable to analyse simpler two-dimensional (2D) manganites such as $La_{1-x}Sr_{1+x}MnO_4$, while the discussion of three-dimensional compounds such as $La_{1-x}Sr_xMnO_3$ will be postponed to the next paper. Indeed, this former class of compounds provides one of the best examples of the complexity of manganite physics. Their experimental properties demonstrate a competition between the electronic interactions and the coupling to the lattice in the presence of finite crystal field splitting of e_g orbitals due to their 2D geometry [17–21].

The paper is organized as follows. Firstly, we introduce a *realistic* model for e_g electrons in monolayer manganites which includes the electron interactions and the local potentials due to JT distortions (section 2). In this section we also introduce the method to treat electron correlation effects beyond the Hartree–Fock (HF) approximation. The numerical results are presented and analysed in section 3. Next, in section 4 we address the question of which parameters of the effective Hamiltonian are the most important ones to account for the experimentally observed situation. Finally, section 5 summarizes the paper and gives general conclusions.

2. The effective model Hamiltonian

We study strongly correlated electrons in undoped and half doped monolayer manganites $La_{1-x}Sr_{1+x}MnO_4$ (with $x = 0$ or 0.5), using an effective model describing only Mn sites, where the state of surrounding oxygens is included by an effective potential at each site. A realistic effective Hamiltonian which acts in the subspace of low energy e_g states can be derived by a procedure of mapping the results of HF, or LDA + U, or all-electron *ab initio* calculations obtained within a more complete approach. A local basis at each manganese site is given in such a model by two Wannier orbitals of the e_g character (of $x^2 - y^2$ and $3z^2 - r^2$ symmetry) [13]. The exact procedure of mapping and the expectations we put onto such an effective model were never precisely defined. Therefore, at present not much is known about the values of the effective Hamiltonian parameters. Their estimation by various authors can be quite different as the effective Hamiltonian can be derived in different contexts (i.e. for the description of different experiments). It is however clear that the 'bare' atomic parameters for Mn ions are not applicable.

After stressing this point, we will pass to presenting the effective model, which, in our opinion, is a necessary compromise between simplicity and the requirement of including all basic and relevant effects responsible for the physical properties of monolayer $La_{1-x}Sr_{1+x}MnO_4$ compounds. We assume that the t_{2g} orbitals of Mn^{3+} ions are occupied by three 'core' electrons with total spin $S = 3/2$—the core electrons are treated here as classical and frozen. Thus, the active electrons which remain are only e_g ones. This approximation for 3/2 core spins was found earlier to perform quite well [2, 11].

We investigate the system by using a 2D Hamiltonian $\mathcal{H}$ (adequate for an ab plane of a monolayer manganite) of Hubbard type

$$\mathcal{H} = H_{\rm kin} + H_{\rm cr} + H_{\rm int} + H_{\rm spin} + H_{\rm JT}, \tag{1}$$

which consists of the kinetic energy $H_{\rm kin}$, the crystal field splitting $H_{\rm cr}$, on-site Coulomb interactions $H_{\rm int}$, spin interactions $H_{\rm spin}$ and the JT part $H_{\rm JT}$. The simplified crystal field term has to be included as one expects a finite anisotropy between two e_g states in the geometry of a monolayer system. This model and/or the essential parts of it were studied earlier in numerous papers [1, 3, 6, 12, 13, 22, 23].

The kinetic part $H_{\rm kin}$ is expressed using the basis of two e_g orbitals

$$x^2{-}y^2 \sim |x\rangle, \qquad 3z^2{-}r^2 \sim |z\rangle, \tag{2}$$

or in brief notation x and z orbitals per site, with anisotropic phase dependent hopping [24],

$$H_{\rm kin} = -\tfrac{1}{4}t_0 \sum_{ij\sigma} \left[3d^\dagger_{ix\sigma} d_{jx\sigma} + d^\dagger_{iz\sigma} d_{jz\sigma} \pm \sqrt{3}(d^\dagger_{ix\sigma} d_{jz\sigma} + d^\dagger_{iz\sigma} d_{jx\sigma}) \right]. \tag{3}$$

Here $d^\dagger_{i\mu\sigma}$ are creation operators for an electron in orbital $\mu = x, z$ with spin $\sigma = \uparrow, \downarrow$ at site i, and $n_{i\mu\sigma} = d^\dagger_{i\mu\sigma} d_{i\mu\sigma}$ are the corresponding electron number operators. The effective Mn–Mn hopping matrix elements arise due to the hybridization with oxygen orbitals on Mn–O–Mn bonds, and are therefore anisotropic and orbital dependent [24]. The sum runs over all pairs of nearest neighbour sites i and j and the $\pm$ is interpreted as a plus sign for the bond $\langle ij \rangle$ being parallel to the crystal axis a and a minus sign for the bond $\langle ij \rangle$ being parallel to the crystal axis b. The kinetic energy is supplemented by the crystal field part

$$H_{\rm cr} = \tfrac{1}{2}E_z \sum_{i\sigma} (n_{iz\sigma} - n_{ix\sigma}). \tag{4}$$

For the present convention, for negative values of crystal field parameter ($E_z < 0$) the z orbital is favoured over the x orbital, as expected for $La_{1-x}Sr_{1+x}MnO_4$ compounds.

The electron interactions are given by [25]

$$H_{\rm int} = U\sum_{i\mu} n_{i\mu\uparrow}n_{i\mu\downarrow} + (U - \tfrac{5}{2}J_{\rm H})\sum_{i} n_{ix}n_{iz} - \tfrac{1}{2}J_{\rm H}\sum_{i}(n_{ix\uparrow} - n_{ix\downarrow})(n_{iz\uparrow} - n_{iz\downarrow}) - J_{\rm H}\sum_{i\mu} S_i^z(n_{i\mu\uparrow} - n_{i\mu\downarrow}), \quad (5)$$

and the spin superexchange part is

$$H_{\rm spin} = J'\sum_{\langle ij\rangle} S_i^z\, S_j^z, \quad (6)$$

with $J' > 0$. In contrast to equation (3), the sum over bonds $\langle ij\rangle$ includes each pair of nearest neighbour sites only once. Here the on-site Coulomb interaction element is denoted as U, Hund's exchange interaction is $J_{\rm H}$, and J' stands for the superexchange interaction between frozen core t_{2g} electrons [3, 15, 23–25]. The Hund's term, as given above in equation (5), is in fact a rather crude approximation. Namely, for simplicity we adopt here the Ising approximation instead of the spin–spin scalar product, i.e. we take the product of two z-components of spin only. Thus, we explicitly break spin rotational symmetry and fix the quantization axis along the z spin component. This approximation follows in the mean field (MF) treatment of the $SU(2)$ symmetric Heisenberg term and significantly simplifies the computation of the correlation energy. On the other hand, the price we must pay is that the phases with space varying local spin quantization axis (such as spiral phases) are excluded from our considerations from the start. As mentioned above, the frozen t_{2g} core spins in equations (5) and (6) are replaced by discrete classical Ising variables $S_i^z = \pm 3/2$ [11, 12].

Finally, the JT part is

$$H_{\rm JT} = \sum_i \left[g(Q_{2i}\tau_i^x + Q_{3i}\tau_i^z) + \tfrac{1}{2}K(Q_{2i}^2 + Q_{3i}^2)\right], \quad (7)$$

where the pseudospin operators τ_i^α (at site i) are

$$\tau_i^x = \sum_\sigma (d_{ix\sigma}^\dagger d_{iz\sigma} + d_{iz\sigma}^\dagger d_{ix\sigma}), \qquad \tau_i^z = \sum_\sigma (d_{ix\sigma}^\dagger d_{ix\sigma} - d_{iz\sigma}^\dagger d_{iz\sigma}), \quad (8)$$

and $\{Q_{2i}, Q_{3i}\}$ denote the active JT deformation modes of the oxygens around a given Mn ion at site i—they lift out the degeneracy of e_g orbitals. For simplicity, fully symmetric (breathing mode) deformation Q_{1i} is neglected in $H_{\rm JT}$, as well as minor, secondary quadratic couplings (for a more elaborate form of $H_{\rm JT}$ as applied to manganites see for example [22, 26]).

The parameters we used for the numerical calculations were taken from the literature. In some cases they are only an educated guess, presumably applicable to monolayer manganites. Thus we take an effective $(dd\sigma)$ hopping element $t_0 = 0.4$ eV following [7], while other estimations in the literature fall in the range 0.2–0.6 eV [1, 4, 27]. The effective on-site Coulomb repulsion will be fixed at an experimental value $U = 2.8$ eV deduced by Kovaleva *et al* [30], but we note that more recent theoretical analysis of the optical spectral weights using an effective spin–orbital model suggests a larger value $U = 5.0$ eV [8]. Here the data used in the literature are widely scattered, as the screening of the atomic value is considerable and U is difficult to estimate. The smallest value is 1.7 eV [13] obtained for the effective model neglecting Hund's exchange interaction. Park *et al* estimated U to be about 3.5 eV using photoemission data [14] (for the undoped perovskite $LaMnO_3$), while a much smaller value ∼2.0 eV was deduced earlier by Okimoto *et al* [28] from the optical conductivity data (for lightly doped $La_{1-x}Sr_xMnO_3$). Other values suggested in the literature are close to 5.0 eV [8, 12], or to 5.5 eV [7] and are likely to be somewhat overestimated.

Coming to Hund's exchange coupling $J_{\rm H}$ we notice that it is widely believed that $J_{\rm H}/t_0$ is larger than unity, and most probably $J_{\rm H}$ is smaller than 1.0 eV [1]. Various authors provide

slightly different values, with J_H varying from the atomic value of 0.9 eV [29] down to 0.7 eV [7] and 0.67 eV [8]. We will take here $J_H = 0.5$ eV, again following [30] and assuming a larger screening, but we note that the ratio of J_H/U, which plays a crucial role for the nature of superexchange interactions [31], is there practically the same as the one given with the somewhat larger electron interaction parameters of [8].

For the JT interaction parameters in equation (7) we take $K = 13$ eV Å^{-2} and $g = 3.8$ eV Å^{-1}, following [4, 32–34]. For the parameter J' in equation (6) we adopted the value 3.0 meV [21], as obtained from the fit to spin-waves in $LaSrMnO_4$. Unfortunately, the fit was performed for the Heisenberg model with nearest neighbour and next nearest neighbour interactions between spins $S = 2$. The actual ratio $J'/t_0 \approx 0.01$ in principle falls into the range 0.01–0.1, which is recommended by Dagotto *et al* in their review article [1]. Still nowadays the opinion is prevailing that J' should be smaller, namely ∼3.0 meV [8] or ∼1.0–1.5 meV [30], but even values as small as 0.4 meV [14] or 0.9 meV were suggested by Millis [4]. Therefore, to be on the safe side we will study the model (1) for three different values of the superexchange, namely $J' = 0$, 1.5, and 3.0 meV. We also included $J' = 0$ to investigate the importance of spin interactions for the observed magnetic order in the undoped and half doped monolayer manganite. As a curiosity let us note that the value of 3.0 meV can be obtained by a simple (but not rigorous) reasoning. Namely, first one computes the MF Néel temperature for the 2D square lattice with AF interactions between $S = 3/2$ core spins $k_B T^0_{MF} = \frac{4}{3} J' \frac{3}{2}(\frac{3}{2} + 1)$, where k_B is the Boltzmann constant and four is the number of nearest neighbours in the ab plane. Then we apply a semiempirical rule relating the MF result with the typical experimental Néel temperature $T^0_{exp} \approx 0.7\ T^0_{MF}$ [35], and insert the experimental value $T^0_{exp} = 127$ K [17, 20]. As a lucky coincidence we obtain for J' virtually the same value as the one given in [21].

As the last parameter we consider E_z, for which we assume the values 0, −0.2, and −0.4 eV. This seems to cover our 'region of interest'. Namely, these values were motivated by the optical gap measurements [17] and by the LDA + U computations. The gap between x and z bands was found to be close to −0.55 eV, which compares well with the −0.4 eV obtained from LDA + U computations performed for $LaSrMnO_4$ [14]. The measurements of the gap do not translate directly into E_z (from our effective Hamiltonian). In fact, the fit done before [15] gives a smaller value, $E_z = -0.12$ eV. Thus, in principle we should study four different E_z values; however, we do more. To be on the safe side in regions of interest we will consider in addition some intermediate values of E_z.

We study 2D square clusters (containing $N = 64$ sites) with periodic boundary conditions, undoped and with hole doping $x = 1 - n = \frac{1}{2}$ away from half-filling ($n = 1$), where n is e_g electron density. First, the calculations within the single-determinant HF approximation were performed to determine the ground state wavefunction $|\Psi_{HF}\rangle$. In the next step the HF wavefunction $|\Phi_0\rangle$ was modified to include the electron correlation effects. We used an exponential local ansatz for the correlated ground state [36],

$$|\Psi\rangle = \exp\Big(-\sum_n \eta_m O_m\Big)|\Phi_0\rangle, \tag{9}$$

where $\delta n_{i\mu\sigma}$ are density fluctuations, and $\{O_m\}$ are correlation operators. The variational parameters η_m are found by minimizing the total energy,

$$E_{tot} = \frac{\langle\Psi|H|\Psi\rangle}{\langle\Psi|\Psi\rangle}. \tag{10}$$

In this way the correlation energy, $E_{corr} = E_{tot} - E_{HF}$, is obtained. For technical details see [23, 37]. For the correlation operators we use

$$O_m = \delta n_{i\mu\sigma}\delta n_{i\nu\sigma}, \tag{11}$$

which stands for the set of all possible $\delta n_{i\mu\sigma}\delta n_{i\nu\sigma'}$ on-site operators (defined separately for each site i). The symbol δ in $\delta n_{i\mu\sigma}$ indicates taking *only that part* of the $n_{i\mu\sigma}$ operator which annihilates one electron in an occupied single particle state from the HF ground state $|\Phi_0\rangle$, and creates an electron in one of the virtual states. The above local operators O_m (11) (in the present model) correspond to the subselection of the most important two electron excitations within the *ab initio* configuration–interaction method. (Three, four, etc, electron excitations are also important in the intermediate and strong correlation regime. However, as yet there is no controlled method implementing them for larger systems).

For a given filling the HF computations were run starting from several (different) initial conditions, i.e., from predefined charge, spin configuration, predefined pattern of core t_{2g} spins and a predefined set of $\{Q_{2i}, Q_{3i}\}$ variables. For each fixed set of initial conditions on convergence we obtain the HF energy $E_{\rm HF}$ and the HF wavefunction $|\Phi_0\rangle$, which were next used to recompute the (renormalized) set of $\{Q_{2i}\}$ and $\{Q_{3i}\}$. The obtained (new) JT deformations $\{Q_{2i}\}$ and $\{Q_{3i}\}$ were then inserted into the HF Hamiltonian again, and this procedure was repeated until JT distortions had converged. This self-consistent procedure was used to provide a local energy minimum with respect to $\{Q_{2i}, Q_{3i}\}$ variables. Then, after finishing such a single self-consistent HF run extended by the computation of $\{Q_{2i}, Q_{3i}\}$ variables (still for the same set of initial conditions), we performed correlation computations (see above) obtaining the total energy $E_{\rm tot}$ (10). Next, such a procedure was applied to a second set of HF initial conditions to determine the local energy minimum E for this configuration. In this way we treated the entire set of initial conditions used in the present calculations. Finally, the resulting set of energies $\{E_n\}$ for different locally stable states was inspected and the lowest energy E_0 and this state was identified as a good candidate for the true ground state for given parameters (we recall that this is the zero temperature ground state).

3. Results in the 'realistic' regime of parameters

3.1. Numerical details

In general the computations are costly and time consuming. We used more than 100 different initial conditions for each set of Hamiltonian parameters, and, as we have found (*a posteriori*), any smaller number would certainly not suffice to cover all *a priori* possible states. This big number corresponds to many potential possibilities. The first possibility is related to the question of whether the e_g electrons in the ground state are all ferromagnetic (FM), i.e. all spins pointing upwards, or if the number of up and down electrons is equal (zero total magnetization). For each of these possible configurations we need separate HF and correlation calculations. For the former case we use the set of about 40 different initial conditions while for the latter one the set of 60. The second factor is the assumed and fixed configuration of core t_{2g} spins. Here we used only a few possibilities: FM, antiferromagnetic (AF) phase staggered along a and b axes (G-type antiferromagnet, so-called G-AF phase), zigzag CE-type [19]; C-AF configuration (vertical FM order with AF coupling between the alternating lines of up and down spins), and similar C-AF-like phase with alternating double lines of up and down spins, respectively, called below the C-AF2 phase. Other possibilities were not taken into account (though certainly examination of some random arrangements of core spins could be of interest in the doped regime with $x \neq 0.5$).

After fixing a core spin configuration, various starting configurations of e_g spins (FM, AF, vertical stripes, diagonal stripes, some random arrangements) were tested, as well as various configurations of $\{Q_{2i}\}$ and $\{Q_{3i}\}$ variables (uniform zero, uniform nonzero, non-zero chequerboard-like, random, etc). Notably, the direction of e_g spin was found to be parallel to

that of the core spin at each site as long as $J_H = 0.5$ eV. This observation allowed us to reduce the numerical effort. Virtually each set of initial conditions leads to some metastable state, but about half of the obtained states have their energies distinctly separated from the remaining manifold of 'metastable' states with lower energies. In the latter low-energy manifold e_g and t_{2g} spins are parallel to each other, and the ground state energy is almost degenerate with several other 'metastable' states. In such a case the identification of the true ground state turns out to be somewhat problematic. Namely, the change of any of the employed approximations and assumptions can (in principle) reverse the order of the ground state with one of the neighbouring 'metastable' states. Take, for example, the assumption that the core spins are frozen. One can easily imagine that unfreezing them could bring a change of the ground state energy of the order of 0.01%, which would be just enough to trigger the discussed crossover. The same holds true for (i) some better treatment of electron correlations, (ii) including weak nearest neighbour intersite Coulomb repulsion, (iii) including next nearest neighbour hopping, and finally (iv) including more elaborate JT couplings (e.g. as used in [26]).

To make the situation worse, the convergence of JT iterations is, in general, rather poor. (We set as the criterion of the HF convergence the energy change by 10^{-6} eV and we assumed that JT self-consistency was reached when during one iteration all $\{Q_{2i}\}$ and $\{Q_{3i}\}$ variables changed by less than 0.001 Å.) Therefore, one could not construct the entire phase diagram, clearly this would be numerically too expensive. Only isolated points of the phase diagram were inspected instead.

3.2. Undoped compound $LaSrMnO_4$

The magnetic structure of $LaSrMnO_4$ reported in several experiments is a G-AF phase [18, 20, 21]. The role played by the JT distortions is experimentally unclear. There exist numerous experiments (in doped and undoped monolayer compounds $La_{1-x}Sr_{1+x}MnO_4$), and numerous model computations which arrive at different conclusions concerning the importance of the JT distortions and mixing of x and z orbitals [20–22, 38, 39]. It seems that the x–z mixing is not universal, but only shows some similarity across different classes of compounds. One of the recent papers suggests that the MnO_6 octahedra in $LaSrMnO_4$ [20] are elongated perpendicularly to the plane, in accordance with a majority occupation of the z orbital. We arrived at exactly the same conclusion by varying the parameters in the expected range. Namely, in the studied range of E_z between 0 and -0.4 eV and taking $J' = 3.0$ meV, the ground state is without any doubt G-AF phase, and the core t_{2g} spins are strictly parallel to e_g spins. However, for sufficiently small values of E_z (between 0 and -0.06 eV) the orbital x is occupied instead, and the orbital z is almost empty (see figure 1). Consistently with this electron distribution, the JT distortions are $Q_{2i} = 0$ and $Q_{3i} < 0$. The latter are all large and uniform in space. For E_z in the range between -0.1 and -0.4 eV the situation is reversed—the orbital z is occupied, while the orbital x is unoccupied (see figure 2). Here the JT distortions Q_{3i} are uniform in space, large and positive (while $Q_{2i} = 0$ as before). As the value $E_z = -0.4$ eV is believed to be close to the crystal field in $LaSrMnO_4$, we obtain the same result as reported in [20]. Also Q_{3i} values are positive, which corresponds to the elongation of MnO_6 octahedra.

For the narrow range of E_z between -0.06 and -0.10 eV we still have a G-type antiferromagnet; however, the precise electron density in x and z orbitals is difficult to establish (as is the case for Q_{3i} distortions). Several states are almost degenerate in this region, most of them showing quasi-random (inhomogeneous in space) mixing of x and z accompanied by inhomogeneous in space distribution of positive and negative Q_{3i} distortions. Moreover, the convergence is unusually slow. About 400 JT iterations are still not quite enough to be sure that

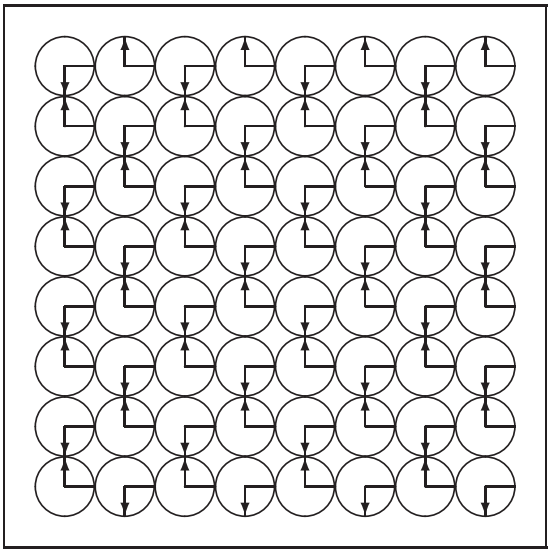

Figure 1. Magnetic, charge and orbital order for e_g electrons as obtained in an 8×8 cluster (with periodic boundary conditions) for the undoped system. Core t_{2g} spins (not shown) are strictly parallel with e_g spins. At each site the circle radius corresponds to e_g on-site total charge; the arrow length to the e_g spin; the horizontal bar length to the charge density difference between $x^2 - y^2$ and $3z^2 - r^2$ orbitals. All these values are expressed in proportionality to the nearest neighbour site–site distance, which is assumed to be unity. Parameters: $t_0 = 0.4$ eV, $U = 2.8$ eV, $J_H = 0.5$ eV, $K = 13$ eV Å^{-2}, $g = 3.8$ eV Å^{-1}, $J' = 3.0$ meV, and $E_z = -0.06$ eV. Additional data: $E_{HF} = -89.1077$ eV, $E_{tot} = -89.1366$ eV. JT distortions (uniform in space, i.e. the same for each site): $Q_{2i} = 0$, $Q_{3i} = -0.29$ Å. Electron densities are $n_x = 0.996$ and $n_z = 0.004$.

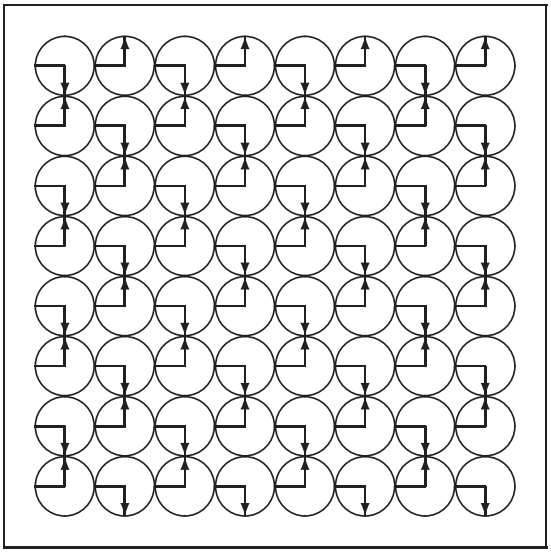

Figure 2. G-AF structure, with z orbitals occupied for $E_z = -0.10$ eV. Legend and other parameters as in figure 1. Additional data: $E_{HF} = -89.5733$ eV, $E_{tot} = -89.5747$ eV. JT distortions (uniform in space): $Q_{2i} = 0$, $Q_{3i} = +0.29$ Å.

JT iterations have indeed converged. Most probably the true ground state corresponds to 1:1 mixing of x and z and uniform in space positive Q_{2i} (see figure 3). Although this parameter

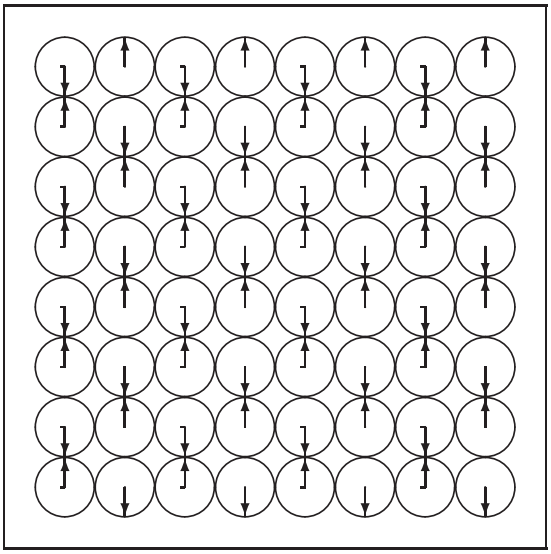

Figure 3. Magnetic, charge and orbital order for $E_z = -0.08$ eV. Legend as in figure 1. Additional information: $E_{\rm HF} = -88.9798$ eV, $E_{\rm tot} = -89.0105$ eV. Uniform in space JT distortions are $Q_{2i} = +0.29$ Å, $Q_{3i} \sim +0.003$ Å.

regime is not relevant for $LaSrMnO_4$, we note that an alternating orbital order of this type would help to stabilize the A-AF phase in $LaMnO_3$ [7].

3.3. Half doped $La_{1-x}Sr_{1+x}MnO_4$ with $x = 0.5$

Next we consider the half doped $La_{0.5}Sr_{1.5}MnO_4$ compound with standard parameters. As before we include the AF superexchange between t_{2g} spins of $J' = 3.0$ meV. For small values of crystal field, namely for E_z in the range from 0 down to -0.12 eV, the ground state is FM with chequerboard-like CO as shown in figure 4. When the crystal field parameter is further decreased to $E_z = -0.14$ eV, the numerical results suggest that the FM ground state disappears (i.e. becomes metastable, with energy -49.469 eV). The 'true' ground state has energy -49.520 eV and has a pronounced chequerboard-like CO. The e_g spins on charge majority sites are organized according to the C-AF pattern; see figure 5.

We could not conclude whether the order displayed in figure 5 is the actual ground state as the next possible candidate is energetically quite close, i.e. with the total energy -49.497 eV (figure 6). This latter state is characterized by similar CO and has e_g spins arranged (on charge majority sites) on diagonal, up and down FM lines. The core spins (not shown) are arranged in a zigzag CE pattern [19]; the directions of core and e_g spins on charge majority sites do agree. We remark that there is also a third phase not too far away, but we will discuss this in the following.

For the crystal field parameter $E_z = -0.16$ eV the phase order situation is similar to that one found for $E_z = -0.14$ eV. However, for still lower $E_z = -0.18$ eV the situation turns out more complicated. Before that we had two almost degenerate states with different types of order, being candidates for the ground state. Now the third one also competes with the other two. To be more specific we have found (i) CO with C-AF order with cluster energy -49.382 eV, (ii) CO + CE magnetic order with cluster energy -49.343 eV, and (iii) stripe-like CO with alternating lines of up and down e_g spins in C-AF phase (figure 7) with cluster energy

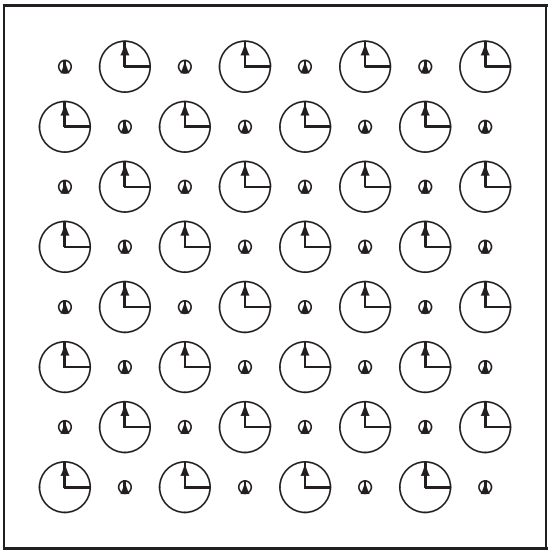

Figure 4. Magnetic, charge and orbital order for half doped compound in the FM phase, as obtained for $E_z = -0.12$ eV. Legend and parameters as in figure 1. JT distortions are $Q_{2i} \sim 0$ (0.015 and 0.003 Å on charge majority and charge minority sites) and $Q_{3i} = -0.23$ (-0.025) Å on charge majority (minority) sites (tetrahedra are shortened along the crystal c axis). Total e_g spin magnitudes on charge majority/minority sites are 0.4/0.1. Note that each figure was automatically generated by the numerical program as a LaTEX file. The LaTEX has only a limited set of predefined circles, thus the circle radii are approximate. In fact major and minor charges are 0.8 and 0.2, respectively. The electrons occupy x orbitals, with a small admixture of z. The cluster HF energy is $E_{\rm HF} = -49.7188$ eV while the total energy is $E_{\rm tot} = -49.7496$ eV. The best metastable state with total zero e_g magnetization has energy -49.648 eV, i.e. is not very well separated from the FM ground state. (The corresponding numbers for $E_z = 0$ are -51.457 and -51.117 eV; i.e., in contrast to the present situation they are reasonably well separated.)

-49.375 eV (this phase is intermediate between cases (i) and (ii)). Note that the stripe-like phase (iii) was also present for $E_z = -0.14$ eV. For $E_z = -0.20$ eV and for $E_z = -0.30$ eV the triad of the ground state candidates still persists, with stripe-like CO phase being the most stable one. Finally, for $E_z = -0.40$ eV (the value believed to be close to the true crystal field parameter) stripe-like CO phase is no longer the best candidate for the ground state (-51.075 eV) and at the top are classical CO + C-AF magnetic order like that in figure 5 (-51.171 eV) and classical CO + CE magnetic order (-51.155 eV), like that in figure 6.

Notably, our simplified effective model (1) gives qualitative results close to the experiment. The chequerboard-like CO we obtained for half doping agrees reasonably well with the neutron and x-ray data (see [21] and earlier papers cited therein). Chequerboard-like CO turns out to be a quite robust feature of the model, emerging for practically any reasonable set of Hamiltonian parameters, as long as the JT coupling parameter g is finite. The obtained amplitude of charge modulation between charge majority and charge minority sites is, however, much larger than that obtained in the experiment [21]. We note that the definition of local charge centred at a given Mn ion is not unique. While the experiment gives information about atomic charges, the d states in the present model represent not just individual Mn ions but rather Wannier orbitals centred on them. It may be expected that each Wannier orbital extends not only up to neighbouring oxygens but up to other Mn ions as well. In other words, in the present effective model (1), charge differences between different Wannier orbitals can be large, but when this is

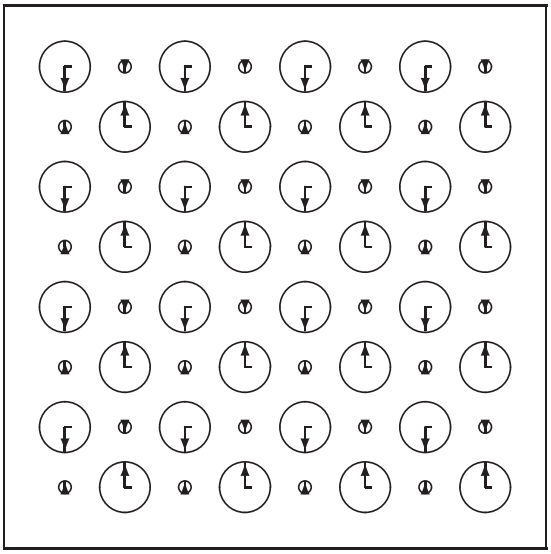

Figure 5. Charge order accompanied by C-AF order in half doped compound for $E_z = -0.14$ eV. Legend and parameters as in figure 1. The x orbital and z orbital occupations on charge majority sites are roughly in the ratio 5:3. Additional information: $E_{\rm HF} = -49.4901$ eV while the total energy is $E_{\rm tot} = -49.5202$ eV; e_g electron densities on charge majority/minority sites are 0.825 and 0.174, respectively. Magnetic moments are ± 0.411 (charge majority) and ± 0.082 (charge minority). Jahn–Teller distortions are $Q_{2i} = -0.226$ Å on charge majority sites and -0.049 Å on charge minority sites; Q_{3i} are negligible ($-0.06/-0.026$ Å on charge majority/minority sites).

translated to real space the charges on Mn ions would be smeared out and the charge variation would be smaller.

Coming to magnetic order, we note that it is widely believed to be of the zigzag CE type (see [21] and references cited therein). However, a glassy magnetic phase in this range of doping was also reported [18]. This is not an experimental contradiction, but rather reflects the well known fact that differently prepared samples under examination can provide different results. Differently phrased, it seems that the true Hamiltonian (and in parallel the phase situation in a real compound) is very sensitive to some secondary factors. This sensitivity has also been found in the present model at half doping ($x = 0.5$).

4. Which parts of the Hamiltonian are the most relevant ones?

An interesting question we would like to address in the context of the above numerical results concerns the relevance of different parts of the model Hamiltonian (1), i.e., which interactions are crucial for the proper description of $LaSrMnO_4$ and $La_{0.5}Sr_{1.5}MnO_4$, and which ones are only of secondary importance. Taking the complexity of the microscopic model (1) one would like to make simplifications and to keep only the essential terms. Indeed, different authors assigned different relevance to on-site Coulomb interactions, to the AF superexchange between core spins, and to the JT coupling to the lattice, and neglected one of these terms [1, 3, 6, 12, 15, 22, 40]. A satisfactory answer to the question of whether simplifications of the Hamiltonian (1) are allowed and could lead to reasonable agreement with the experiment calls for construction of the phase diagrams for all possible regimes of Hamiltonian parameters. Unfortunately, within the present approach we cannot afford such

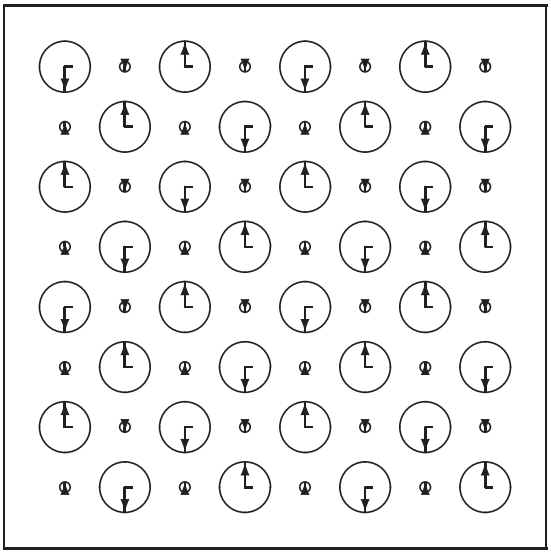

Figure 6. A metastable state with energy very close to the ground state, exhibiting CO accompanied by CE magnetic order for half doped compound at $E_z = -0.14$ eV. CE order refers to the total ($t_{2g} + e_g$) spins. (Note that on charge majority sites the e_g spins are arranged on diagonal lines.) Legend and parameters as in figure 1. The magnetic moments of e_g electrons are ± 0.411 and ± 0.082 on charge majority/minority sites. JT distortions of the Q_{2i} type on charge majority sites are 0.229 Å (for up spins) and -0.229Å (for down spins); on charge minority sites they are zero. JT distortions of the Q_{3i} type are negligible ($-0.073/-0.026$ Å on charge majority/minority sites). The x to z occupation on charge majority sites is roughly 5:3, while on charge minority sites it is roughly 3:1. $E_{\rm HF} = -49.4386$ eV while the total energy is $E_{\rm tot} = -49.4966$ eV.

large scale and overcostly computations. Still, some test computations have been conducted and they clarify the situation to some extent.

First of all, decreasing the AF superexchange interaction between core spins to $J' = 1.5$ meV does not influence the solutions in any significant way. Qualitatively, the types of order obtained then in the ground states for $E_z = 0$, -0.12, -0.20, and -0.40 eV are exactly the same as those found for $J' = 3.0$ meV. Of course, there are some quantitative changes which would be of importance for an accurate comparison with the experiments for $La_{0.5}Sr_{1.5}MnO_4$, but the present model is more appropriate for a qualitative discussion. For zero crystal field and for $E_z = -0.12$ eV the ground state of a half doped monolayer is FM with chequerboard CO state, and with x orbitals occupied (as in figure 4). It changes to stripe-like CO (exactly the same as that in figure 7) when E_z is decreased to -0.20 eV. The energy for the considered 8×8 cluster is then -49.399 eV, actually quite close to the energy of -49.336 eV found for the chequerboard CO state accompanied by the magnetic zigzag-like CE order. The x and z orbitals are occupied in the ratio 1:1 in this latter state. Finally, for $E_z = -0.40$ eV the ground state (with energy -51.171 eV) is the chequerboard CO state with C-AF order (compare figure 5), and only z orbitals are occupied. Then close to it (at energy -51.156 eV) we have found chequerboard CO plus magnetic zigzag-like CE (only z orbitals occupied); next chequerboard+ C-AF2 magnetic order (with energy -51.133 eV); next stripe-like CO + C-AF order (with energy -51.075 eV). Thus, if the crystal field value is indeed close to $E_z = -0.40$ eV, then it is difficult to decide which value of the superexchange parameter is more realistic, $J' = 1.5$ or $J' = 3.0$ meV, using the energy considerations alone. In this respect magnetic measurements, accompanied by a careful analysis of the microscopic parameters, are necessary.

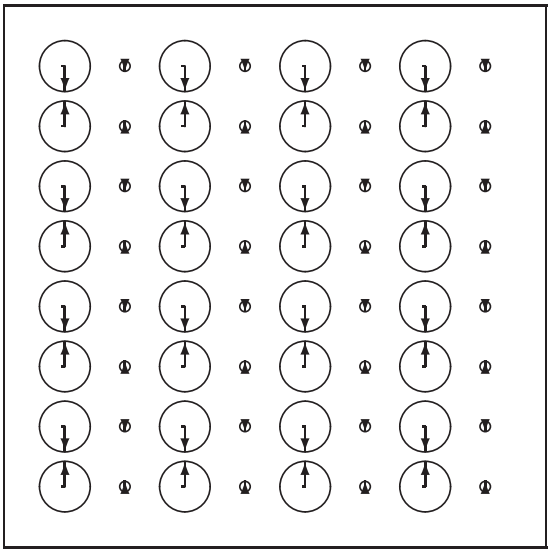

Figure 7. Stripe-like CO plus C-AF magnetic order (metastable state very close to the ground state), obtained for half doped compound and $E_z = -0.18$ eV. Legend and parameters as in figure 1. Electron densities on charge majority/minority sites are 0.822 and 0.178, respectively, while the corresponding magnetic moments are ± 0.410 and ± 0.088. JT distortions on charge majority sites are $Q_{2i} = -0.238$ Å (-0.046 on charge minority sites). Q_{3i} are negligible ($+0.032$ and -0.023 on charge majority/minority sites). The energies are $E_{\rm HF} = -49.3654$ eV and $E_{\rm tot} = -49.3751$ eV.

We also considered the case without superexchange interactions, $J' = 0$. For the undoped monolayer the neglect of Heisenberg interaction between core spins leads immediately to disagreement with the experiment, at least in the case of finite negative crystal field, as expected for $LaSrMnO_4$. For degenerate e_g orbitals ($E_z = 0$) the ground state is pure x type, accompanied by G-AF order just as before. For negative $E_z = -0.20$ or -0.40 eV, z orbitals are occupied instead, again as before. However, now the spin order is quite different. Namely, one finds C-AF phase (similar to figure 5 but for homogeneous charge distribution). For $E_z = -0.12$ eV the magnetic order resembles the C-AF one, but is instead characterized by alternating double FM lines of up and down spins, respectively; we denoted this order above as C-AF2. Such states were not observed in the real compounds. Therefore, we conclude that finite AF superexchange interaction $J' > 0$ is essential to suppress the generic tendency towards FM order along one lattice direction, which persists even for relatively large negative values of $E_z \sim 0.40$ eV.

For half doped substance the neglect of Heisenberg interaction of core spins J' leads again to the results concerning the magnetic order which contradict the experiments. For all crystal field values considered here we obtained an ideal FM order in the ground state (for aligned e_g and t_{2g} core spins), accompanied by CO of chequerboard type. For crystal field up to -0.12 eV only x orbitals are occupied. For $E_z = -0.20$ eV one obtains a variant of the previous state, namely the CO with only roughly classical chequerboard order. There are two different charge majority sites with charges in proportionality 2:1. One vertical row of the atoms (bigger charges) shows only z occupation, the second (neighbouring) vertical raw (smaller charge) shows only x occupancies, and then the pattern repeats. For $E_z = -0.40$ eV this variant disappears and again we obtain ideal FM+checkboard CO order with only z orbitals occupied.

We also performed calculations neglecting the JT effect, i.e. taking $g = 0$. Such a simplification of the model results in very efficient calculations when the self-consistency over the lattice distortions $\{Q_{2i}, Q_{2i}\}$ can be avoided, but is also not allowed. Namely, for zero crystal field one finds then ideally aligned FM phase with equal occupation of x and z orbitals. This state, although not relevant for the physical situation in $LaSrMnO_4$, could describe (in the presence of AF superexchange coupling along the c axis) an FM ab plane in the A-AF phase of $LaMnO_3$. In fact, it shows that superexchange interactions due to e_g and t_{2g} electrons alone could induce the observed magnetic order in the undoped $LaMnO_3$, but the temperature of the structural transition would then be only about half of the experimental value [7]. In contrast, for $E_z = -0.20$ eV (and $g = 0$) only z orbitals are occupied and the magnetic order is C-AF2, while for $E_z = -0.40$ eV we obtain uniform charge distribution plus magnetic zigzag CE phase (for both core spins plus e_g spins) as the magnetic ground state. This demonstrates that the JT interactions are here even more important than in cubic manganites.

Also for the doped substance the neglect of the JT coupling is not permissible. We have verified that when the JT coupling is neglected, one obtains basically FM ground state with uniform charge distribution and equal electron density in x and z orbitals at each site. There would be some minor modifications to this simple picture but they are only of secondary importance and can safely be neglected when comparing such states with experimental data. Namely, for $E_z = 0, -0.12, -0.20$ eV a tiny diagonal modulation is superimposed on uniform charge background. Each second diagonal line carries slightly bigger charges and a fractionally bigger electron occupancy of x orbitals. The diagonal lines in between have equal electronic density within x and z orbitals and smaller overall charges. The total e_g spins are uniform in space and small (they correspond to those allowed by smaller charge densities of e_g electrons per site). Finally, for $E_z = -0.40$ eV the occupation of x and z orbitals is the same everywhere (on each site) and only a tiny charge modulation develops in the form of vertical stripes (two lines thick).

Next, we neglected Hund's exchange J_H between e_g electrons and superexchange interactions of core spins J'. Although this assumption is expected to be unrealistic, here we will test still another possibility suggested recently in [15]. The idea is that, at least in principle, it could be that the electron correlations are only of secondary importance and that the JT coupling accompanied by the crystal field splitting in a 2D geometry dominate and are already sufficient to describe the phase situation in monolayer manganites. If electronic interactions could be entirely neglected, the problem would simplify tremendously as the electronic Hamiltonian would then reduce to a quadratic form, which could be diagonalized for any choice of the effective fields induced by the JT distortions. This concept is already quite old and popular in the field—it was discussed *in extenso* by Dagotto *et al* in their review article [1]. In fact we do not attempt to present here a polemic discussion with this approach, but will simply use some of the Hamiltonian parameters provided there and discuss the results.

Thus, following [15], we assign to U a small value of $U = 1.12$ eV (which stands here for intermediate on-site Coulomb interaction), corresponding to $U/t_0 = 1.7/0.6$ in [15] (which in our case gives the above value when $t_0 = 0.4$ eV). We also adopt the value of $E_z = -0.12$ eV for the crystal field splitting (but we also considered a second value, i.e. -0.20 eV). Furthermore, we assume that the JT parameters g and K take the established values which we have already studied in this paper. Hund's exchange interaction J_H and the superexchange interaction J' are put to zero again following [15].

Surprisingly, this approach seems to work reasonably well, at least at the beginning. For the undoped monolayer we obtain homogeneous charge distribution and simple G-AF order. Magnetic moments of e_g electrons are of the order of 0.3, while $Q_{2i} = \pm 0.24$ and $Q_{3i} = -0.16$ Å. The ratio of x orbital to z orbital occupations is then close to 3:1 (for

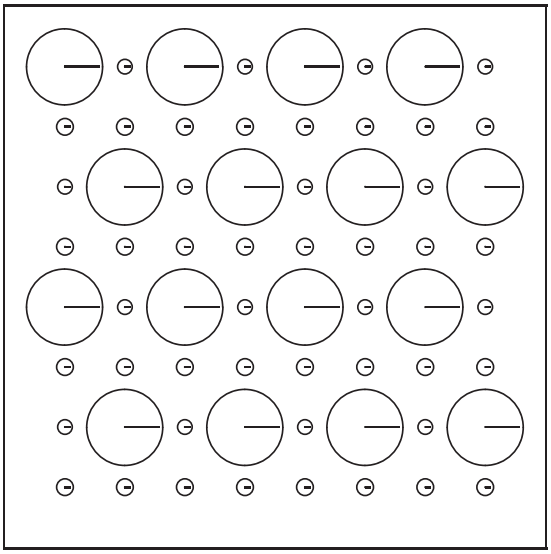

Figure 8. Exotic charge order for half doped compound as obtained in the absence of the AF superexchange, $J' = 0$. Other parameters: $t_0 = 0.4$ eV, $U = 1.12$ eV, $J_{\rm H} = 0$, $K = 13$ eV Å^{-2}, $g = 3.8$ eV Å^{-1}, and $E_z = -0.12$ eV.

$E_z = -0.20$ eV the corresponding ratio is modified to 1:1). However, this choice of parameters leads to an unrealistic description at half doping $x = 0.5$, where one obtains robust CO accompanied by the absence of the magnetic order, which does not resemble the experimental results for $La_{0.5}Sr_{1.5}MnO_4$ (see figure 8). First of all, the CO is not chequerboard-like, and secondly, magnetic moments do not form, i.e. one finds a *nonmagnetic ground state*. On charge majority sites Q_{3i} distortions are small, while Q_{2i} ones are large and positive. As the charge flows almost completely to the majority sites, the JT distortions $\{Q_{2i}, Q_{3i}\}$ cannot form and are negligible on charge minority sites.

The phase situation for larger crystal field splitting at $E_z = -0.20$ eV is looking even more strange, while for $E_z = -0.40$ eV any type of magnetic order vanishes and the CO takes the form of high charge, low charge vertical lines in a stripe phase (similar to that from figure 7, only the high/low charge variation is much smaller). Therefore, we conclude that strong Coulomb interaction $U/t_0 \sim 5$, and considerable Hund's exchange $J_{\rm H}$, as included in more realistic recent LDA + U electronic structure calculations [16], are essential for the observed ground state of half doped monolayer manganites. Intermediate (or small) U will not suffice to form the chequerboard-like CO in half doped manganites, while the exchange interactions ($J_{\rm H}$ and J') are crucial to obtain the AF states observed in the experiment.

5. Summary

We have analysed an effective theoretical model (1) for monolayer manganites. It includes all essential features of e_g electrons, such as their anisotropic phase dependent hopping, large on-site electron interactions described by the Coulomb U and Hund's exchange $J_{\rm H}$, and the coupling of e_g electron spins to frozen spins of core t_{2g} electrons at Mn ions. The state of e_g electrons is also influenced by the crystal field splitting in the 2D geometry of a monolayer, and by the distortions of the surrounding oxygens, which we treated self-consistently with the

electronic problem. We could not provide a precise proof but rather gave many arguments supporting the claim that all these interactions enter on equal footing and play an essential role for the correct interpretation of the experimental data, both for undoped and for half doped compounds.

For the case of undoped substance (in agreement with the experiment) we have found a G-AF ground state with z orbitals occupied and uniform JT elongation of MnO_6 tetrahedra along the c axis perpendicular to the manganese ab plane. The appearance of this phase seems to be robust, as it is found for any reasonable set of the Hamiltonian parameters. Similarly so, the chequerboard CO for half doped substance is also a robust feature of the discussed model (1), but only in the presence of the JT coupling. The CO could be here responsible for novel solitonic effects [41] and could be the mechanism which drives the observed robust orbital order [42], accompanied by the CE magnetic order [43].

However, the magnetic order (superimposed on CO at half doping) was found to be very sensitive to the details of the model. Although the correct CE phase was found to be a good candidate for the true ground state, we also found other candidates such as C-AF order in the immediate neighbourhood in the parameter space. Indeed, in the absence of the JT effect both phases strongly compete and may even become almost indistinguishable from each other when J' is small [12]. Although we do not intend to claim that we have completely clarified the situation, the picture emerging from the great number of performed test computations is that magnetic order in the half doped monolayer does not originate from a single and universal electronic mechanism, but rather depends on the JT coupling to the lattice, which first drives the orbital instability in the CO state [26], and the magnetic order in the form of FM zigzag stripes (CE phase) follows. It is intriguing whether the JT distortions are also of equal importance for some other phenomena near the degeneracy of e_g orbitals, for instance for the stripes in the doped nickelates, treated so far only in the electronic model [44].

Altogether, we conclude that the effective model (1) performs reasonably well. The joint effect of large Coulomb interactions and of JT interactions with the lattice plays a crucial role in the observed types of magnetic order in the monolayer manganites. This good performance merits the hope that it is worthwhile to make an attempt (in the future) to describe the (technically more demanding) phase situation in bilayer $La_{2-x}Sr_{1+x}Mn_2O_7$ manganites, and in the three-dimensional doped perovskite compounds like $La_{1-x}Sr_xMnO_3$, using the same model Hamiltonian.

Acknowledgment

This work was supported by the Polish Ministry of Science and Education Research Project No 1 P03B 068 26.

References

[1] Dagotto E, Hotta T and Moreo A 2001 *Phys. Rep.* **344** 1
Dagotto E 2005 *New J. Phys.* **7** 67
[2] Weisse A and Fehske H 2004 *New J. Phys.* **6** 158
[3] Hotta T, Malvezzi A L and Dagotto E 2000 *Phys. Rev.* B **62** 9432
[4] Millis A J 1996 *Phys. Rev.* B **53** 8434
Millis A J 1997 *Phys. Rev.* B **55** 6405
[5] Sartbaeva A, Wells S A, Thorpe M F, Božin E S and Billinge S J L 2006 *Phys. Rev. Lett.* **97** 065501
[6] Salafranca J and Brey L 2006 *Phys. Rev.* B **73** 024422
[7] Feiner L F and Oleś A M 1999 *Phys. Rev.* B **59** 3295
[8] Oleś A M, Khaliullin G, Horsch P and Feiner L F 2005 *Phys. Rev.* B **72** 214431
[9] Chibotaru L F 2005 *Phys. Rev. Lett.* **94** 186405

[10] Mizokawa T and Fujimori A 1997 *Phys. Rev.* B **56** R493
[11] Dagotto E, Yunoki S, Malvezzi A L, Moreo A, Hu J, Capponi S, Poilblanc D and Furukawa N 1998 *Phys. Rev.* B **58** 6414
[12] Daghofer M, Oleś A M and von der Linden W 2004 *Phys. Rev.* B **70** 184430
Daghofer M, Oleś A M, Neuber D and von der Linden W 2006 *Phys. Rev.* B **73** 104451
[13] Jung J H, Ahn J S, Yu J, Noth T W, Lee J, Moritomo Y, Solovyev I and Terakura K 2000 *Phys. Rev.* B **61** 6902
[14] Park K T 2001 *J. Phys.: Condens. Matter* **13** 9231
[15] Yin W-G, Volja D and Ku W 2006 *Phys. Rev. Lett.* **96** 116405
[16] Yamasaki A, Feldbacher M, Yang Y-F, Andersen O K and Held K 2006 *Phys. Rev. Lett.* **96** 166401
[17] Moritomo Y, Asamitsu A and Tokura Y 1995 *Phys. Rev.* B **51** 16491
[18] Morimoto Y, Tomioka Y, Asamitsu A, Tokura Y and Matsui Y 1995 *Phys. Rev.* B **51** 3297
[19] Sternlieb B J, Hill J P, Wildgruber U C, Luke G M, Nachumi B, Morimoto Y and Tokura Y 1996 *Phys. Rev. Lett.* **76** 2169
Park J H, Chen C T, Cheong S, Bao W, Meigs G, Chakarian V and Izeda Y U 1996 *Phys. Rev. Lett.* **76** 4215
Wilkins S B, Spencer P D, Hatton P D, Collins S P, Roper M D, Prabhakaran D and Boothroyd A T 2003 *Phys. Rev. Lett.* **91** 167205
Chatterji T, Fauth F, Ouladdiaf B, Mandal P and Ghosh B 2003 *Phys. Rev.* B **68** 052406
Huang D J, Wu W B, Guo G Y, Lin H J, Hou T Y, Chang C F, Chen C T, Fujimori A, Kimura T, Huang H B, Tanaka A and Jo T 2004 *Phys. Rev. Lett.* **92** 087202
[20] Senff D, Rentler P, Braden M, Friedt O, Bruns D, Cousson A, Bourée F, Merz M, Büchner B and Revcolevschi A 2005 *Phys. Rev.* B **71** 024425
[21] Larochelle S, Mehta A, Lu L, Mang P K, Vajk O P, Kaneko N, Lynn J W, Zhou L and Greven M 2005 *Phys. Rev.* B **71** 024435
[22] Popovic Z and Satpathy S 2000 *Phys. Rev. Lett.* **84** 1603
[23] Rościszewski K and Oleś A M 2005 *Phys. Status Solidi* b **243** 155
[24] Zaanen J and Oleś A M 1993 *Phys. Rev.* B **48** 7197
[25] Oleś A M 1983 *Phys. Rev.* B **28** 327
[26] Bala J, Horsch P and Mack F 2004 *Phys. Rev.* B **69** 094415
[27] Bocquet A E, Mizokawa T, Saitoh T, Namatame H and Fujimori A 1992 *Phys. Rev.* B **46** 3771
Chainani A, Mathew M and Sarma D 1993 *Phys. Rev.* B **47** 15397
Arima T, Tokura Y and Torrance J B 1993 *Phys. Rev.* B **48** 17006
Saitoh T, Bocquet A E, Mizokawa T, Namatame H, Fujimori A, Abbate A, Takeda Y and Takano M 1995 *Phys. Rev.* B **51** 13942
[28] Okimoto Y, Kasufuji T, Ishikawa T, Urushibara A, Arima T and Tokura Y 1995 *Phys. Rev. Lett.* **75** 109
[29] Feinberg D, Germain P, Grilli M and Seibold G 1998 *Phys. Rev.* B **57** R5583
[30] Kovaleva N N, Boris A V, Bernhard C, Kilakov A, Pimenov A, Balbashov A M, Khaliullin G and Keimer B 2004 *Phys. Rev. Lett.* **93** 147204
[31] Feiner L F, Oleś A M and Zaanen J 1997 *Phys. Rev. Lett.* **78** 2799
Oleś A M, Horsch P, Feiner L F and Khaliullin G 2006 *Phys. Rev. Lett.* **96** 147205
[32] Kawano H, Kojimoto R, Kubota M and Yoshizawa H 1996 *Phys. Rev.* B **53** R14709
[33] Bala J and Oleś A M 2000 *Phys. Rev.* B **62** R6085
Bala J, Oleś A M and Sawatzky G A 2002 *Phys. Rev.* B **65** 184414
[34] Tyer R, Temmerson W M, Szostek Z, Banach G, Svane A and Gehring G A 2004 *Europhys. Lett.* **65** 519
[35] Fleck M, Zacher M G, Lichtenstein A I, Hanke W and Oleś A M 2004 *Eur. Phys. J.* B **37** 439
[36] Stollhoff G and Fulde P 1980 *J. Chem. Phys.* **73** 4548
Stollhoff G 1996 *J. Chem. Phys.* **105** 227
Fulde P 1991 *Electron Correlations in Molecules and Solids* (*Springer Series in Solid State Sciences* vol 100) (Berlin: Springer)
[37] Góra D, Rościszewski K and Oleś A M 1999 *Phys. Rev.* B **60** 7429
Rościszewski K and Oleś A M 2003 *J. Phys.: Condens. Matter* **15** 8363
[38] Mizokawa T and Fujimori A 1996 *Phys. Rev.* B **54** 5368
[39] Ebata K, Mizokawa T and Fijimori A 2005 *Phys. Rev.* B **72** 233104
[40] Brey L 2005 *Phys. Rev.* B **71** 172426
[41] Brey L and Littlewood P B 2005 *Phys. Rev. Lett.* **95** 117205
[42] Lee Y S, Onoda S, Arima T, Tokunaga Y, He J P, Kaneko Y, Nagaosa N and Tokura Y 2006 *Phys. Rev. Lett.* **97** 077203
[43] Senff D, Krüger F, Scheidl S, Benomar M, Sidis Y, Demmel F and Braden M 2006 *Phys. Rev. Lett.* **96** 257201
[44] Raczkowski M, Frésard R and Oleś A M 2006 *Phys. Rev.* B **73** 094429
Frésard R, Raczkowski M and Oleś A M 2005 *Phys. Status Solidi* b **242** 370